Effect of Pump Flow Mode of Novel Left Ventricular Assist Device Upon End Organ Perfusion in Dogs With Doxorubicin Induced Heart Failure

Kazuhiro Eya, Egemen Tuzun, Jeff Conger, Hyun K. Chee, Denise Byler, Chisato Nojiri, O. H. Frazier, and Kamuran Kadipasaoglu

End organ effects of nonpulsatile (NP) and pulsatile (P) left ventricular assist device (LVAD) flow were compared in a canine model of doxorubicin-induced heart failure. After heart failure induction, a prototype bimodal LVAD was implanted. Hemodynamics, cardiac dimensions, and myocardial metabolism were monitored with the LVAD off (baseline) and on (in NP and P modes at 70% or 100% power). End organ perfusion was assessed by colored microsphere analysis. Seven dogs were used: two died before pump implantation and were excluded from analysis, and the remaining five survived to study termination. At 70% NP, ascending aortic flow and myocardial oxygen consumption (MVO_2) decreased significantly. At 100% NP, LV dimensions decreased, aortic systolic, pulse, and LV pressures decreased but not significantly, and ascending aorta flow reversed. At 100% NP, coronary blood flow, MVO_2, and LV free wall subepicardial and subendocardial blood flows decreased significantly. However, as NP support increased, the subepicardial/subendocardial blood flow ratio remained near baseline. At 100% NP, right ventricular perfusion decreased but not significantly, cerebral perfusion decreased significantly, and renal perfusion stayed constant. P mode results were similar, except that ascending aorta flow decreased significantly at 100% P instead of reversing as at 100% NP. These results suggest that end organ perfusion is not differentially affected by LVAD flow mode during chronic heart failure. *ASAIO Journal* 2005; 51:41–49.

Mechanical circulatory support (MCS) devices have been used successfully as bridges to transplantation,[1] as bridges to myocardial recovery,[2] and as permanent circulatory support[3] in patients with end-stage heart failure. These devices can be classified into two general categories according to the type of flow they generate: pulsatile (P) or nonpulsatile (NP). Several experimental studies have investigated the short- and long-term effects of flow mode upon the microcirculation, metabolism, and physiology of end organs (*i.e.*, the heart, brain, kidney, and liver),[4–7] although these studies have usually been performed in healthy or acutely failing hearts. To our knowledge, no study has yet evaluated the effect of MCS flow mode upon end organs in an appropriate model of chronic dilated cardiomyopathy. In the present study, we assessed the short-term effects of P *versus* NP flow from a prototype left ventricular assist device (LVAD) upon the microcirculation, metabolism, and function of major end organs including the heart in a canine model of doxorubicin-induced chronic dilated cardiomyopathy.

From the Texas Heart Institute at St. Luke's Episcopal Hospital, Houston, Texas.

Submitted for consideration June 2004; accepted for publication in revised form October 2004.

Correspondence: Dr. Kamuran A. Kadipasaoglu, Cardiovascular Research Laboratories, Texas Heart Institute at St. Luke's Episcopal Hospital, P.O. Box 20345, MC 3–147, Houston, TX 77225–0345.

DOI: 10.1097/01.MAT.0000150510.03339.AD

Materials and Methods

Animals

Experiments were conducted on mongrel dogs (n = 7), each weighing 35–40 kg. All dogs received humane care in compliance with the *Principles of Laboratory Animal Care* (National Society of Medical Research) and the *Guide for the Care and Use of Laboratory Animals* (National Institutes of Health publication no. 85–23, revised 1996). Our institution's Animal Care and Use Committee approved all protocols used in this study.

Heart Failure Model

Heart failure was induced as follows. Each dog was premedicated with acepromazine and oxymorphone, placed in a supine position, and intubated for mechanical ventilation. Anesthesia was induced and maintained with isoflurane. The right femoral artery was punctured and threaded with a 6F Judkins catheter. The catheter was then advanced under fluoroscopic guidance into the left main coronary artery. Serial ventriculography and two-dimensional echocardiography were used to evaluate left ventricular (LV) end systolic dimension (LVSd), LV end diastolic dimension (LVDd), and fractional shortening (FS). Doxorubicin (Adriamycin) (0.7 mg/kg) was infused rapidly into the coronary artery through the catheter. This infusion was repeated weekly for 5 consecutive weeks. Hemodynamic status was evaluated periodically. After the last infusion of doxorubicin, each dog was kept in a dedicated animal care facility for 1 week.

Pump Description

A prototype pump (DuraHeart; Terumo, Inc., Minneapolis, MN) was used to provide MCS. The prototype pump and its controller were customized for this particular animal experiment at our institution's request. The pump is a sterile, titanium

centrifugal device containing a magnetically suspended impeller. The customized controller has two sets of analog circuitry, one for magnetic levitation of the impeller and the other for control of the motor's rotational speed. For this particular study, we used a laptop personal computer to control the rotational speed (rpm) in either NP or P mode.

Pulsatile flow was based upon changes in motor speed (sine wave) at a given frequency. In P mode, mean rotational speed, amplitude of pulsatility, and pulse rate can be programmed *via* the external personal computer to create a pulsatile flow. In this study, we programmed the computer to produce P flow at a mean rotational speed of ± 300 rpm (amplitude, 600 rpm) and a pulse rate of 80 bpm. The pump was operated in each mode at 70% and 100% of maximum power (70NP, 100NP, 70P, and 100P, respectively).

Pump Implantation

Each dog was premedicated and anesthetized as described previously in this article and then positioned for left thoracotomy. A Swan-Ganz pulmonary arterial catheter and an arterial cannula were introduced into the left jugular vein and the left common carotid artery, respectively. The chest was entered through the fifth intercostal space, the pericardium was opened, and a 3 mm perivascular ultrasonic flow probe (Transonic Systems, Ithaca, NY) was placed around the left anterior descending (LAD) coronary artery. After intravenous injection of heparin (1 mg/kg), the pump outlet graft was anastomosed end to side to the descending thoracic aorta, and a sewing cuff for the pump inlet was sutured around the LV apex. During pump inlet insertion, myocardial tissue samples were harvested from the LV apex with a coring knife and sent for histopathologic examination. The pump was then implanted, and air was thoroughly evacuated from the system. A 16 mm ultrasonic flow probe was placed around the ascending aorta and a 12 mm probe around the outlet graft. A microtip pressure catheter (Millar PC 500; Millar Instruments, Inc, Houston, TX) was advanced into the left ventricle through the left femoral artery. An 8-Fr Swan-Ganz catheter was inserted into the pulmonary artery *via* the left external jugular vein.

Hemodynamic Assessment

After pump implantation, hemodynamics were allowed to stabilize for 30 minutes. Hemodynamics were assessed with the pump off and the outflow graft clamped to avoid pump regurgitation (baseline) and with the pump operating at the four experimental settings described previously (70NP, 100NP, 70P, and 100P) for 30 minutes at each setting. After each change to a new pump setting, hemodynamics were allowed to stabilize for 10 minutes before collecting hemodynamic data. Heart rate (HR), aortic systolic pressure (AoPs), aortic diastolic pressure (AoPd), mean aortic pressure (AoPm), LV systolic pressure (LVP), LV end diastolic pressure (LVEDP), mean pulmonary artery pressure (PAP), central venous pressure (CVP), and cardiac output (CO) were measured at each setting. Data from 10–20 consecutive beats were averaged and used to derive steady state parameters.

Echocardiographic Assessment

Serial two-dimensional transepicardial studies were performed at each pump setting. Echocardiographic assessment was accomplished using a Hewlett Packard Sonos 2000 ultrasound system equipped with a 2.5 MHz phased array transducer, according to the guidelines of the American Society of Echocardiography.[8] The echocardiogram was used to measure systolic and diastolic LV internal dimensions (LVDs and LVDd); LV, RV, and septal wall motion; and aortic valve motion.

Myocardial Oxygen Consumption Assessment

An 18 gauge angiocatheter was inserted into the coronary sinus to take blood samples at baseline and each experimental setting. These samples were used to assess myocardial oxygen consumption (MVO_2), calculated as

$$MVO_2 = CBF \cdot [\bar{a} - v] \quad (1)$$

where $\bar{a}$ and v are aortic and coronary sinus blood oxygen content, respectively, and coronary blood flow (CBF) is the left anterior descending (LAD) coronary artery blood flow rate. A Novastat Profile M blood gas analyzer (Nova Biomedical Co., Waltham, MA) was used for blood gas analysis.

Regional Blood Flow Distribution Assessment

Regional blood flow distribution to end organs of interest (heart, brain, and kidney) was evaluated by microsphere analysis using 15 μm, nonradioactive, stable isotope-labeled microspheres (BioPAL, Worcester, MA), as described in detail elsewhere.[9,10] The microspheres were injected into the left atrium (LA) immediately before pump implantation (baseline) and 10 minutes after pump operation at each experimental setting (70NP, 100NP, 70P, and 100P). Labeled microspheres appeared as follows: with samarium, black; with gold, red; with iridium, yellow; with lutetium, pink; with rhenium, orange; and with antimony, violet. Each labeled microsphere was used at a different pump setting. Arterial reference blood samples were taken from the left common carotid artery after LA injections and used to normalize tissue sample readings.

A neutron activation technique was used to detect microspheres in tissue samples.[11] This technique consists of first irradiating a sample with neutrons in a nuclear reactor to produce specific radionuclides and then quantitatively measuring by gamma spectroscopy the characteristic gamma rays emitted by the decaying radionuclides. Gamma rays detected at a particular energy are indicative of a specific radionuclide's presence. Data reduction of gamma ray spectra then yields the concentrations of various elements in the samples being studied. Neutron activation is capable of detecting a single microsphere in an intact myocardial sample while providing simultaneous quantitative measurements of multiple isotope labels. This high sensitivity and capability for measuring perfusion in intact tissue are advantages over other techniques, such as optical detection of microspheres. Neutron activation is also an effective technique for reducing the production of low level radioactive waste generated during biomedical research.

At study termination, dogs were euthanized with an intravenous bolus of potassium chloride while still under general anesthesia. The heart, brain, and kidney were then harvested for further analysis of regional blood flow. In the case of the heart, both ventricles were isolated, and both were divided into four equal transverse sections along the atrioventricular

Table 1. Echocardiographic and Hemodynamic Measurements Before and After Heart Failure Induction by Doxorubicin Infusion

	Before First Infusion (Baseline)	After Last Infusion (Before Pump Implantation)	*p*
LVDs (mm)	21.9 ± 1.4	31.5 ± 2.6	0.05
LVDd (mm)	34 ± 2.0	40.4 ± 3.0	0.05
FS (%)	35.5 ± 1.5	22.0 ± 2.3	0.05
HR (bpm)	99 ± 3	115 ± 10	0.05
LVEDP (mm Hg)	6.4 ± 1.8	13.6 ± 2.1	0.05
dp/dt (mm Hg/sec)	2,355 ± 95	2,485 ± 238	NS
PAP (mm Hg)	24.6 ± 1.5	23.2 ± 0.8	NS
CVP (mm Hg)	4.6 ± 0.9	5.2 ± 0.8	NS
CO (L/min)	4.49 ± 0.45	4.17 ± 0.7	NS

Values shown are mean ± SD. CO, cardiac output; CVP, central venous pressure; dp/dt, rate of change in left ventricular pressure over time; FS, fractional shortening; HR, heart rate; LVDd, left ventricular end diastolic dimension; LVDs, left ventricular end systolic dimension; NS, not significant; PAP, pulmonary artery pressure; LVEDP, left ventricular end diastolic pressure.

groove. Basal and apical sections were discarded. The more distal of the remaining two sections was selected. The LV section was then divided into two segments representative of the anterolateral and posterior walls. Then, each segment was further subdivided into an epicardial and an endocardial subregion. Two grams of tissue were taken from each region (a total of four tissue samples) for microsphere analysis. RV blood flow was assessed in three total thickness tissue samples weighing 2 g each.

The left hemisphere of the brain was divided into three equal parts posteroanteriorly, and the middle sections were harvested for microsphere analysis. Two grams of tissue were taken from the cortex and corpus medullare (a total of two samples) for microsphere analysis.

The left kidney was divided into three frontal sections, and the middle section was divided into cortical and medullar subregions. Two grams of tissue were taken from each subregion (a total of two kidney tissue samples) for microsphere analysis.

All tissue samples were dried overnight at 70°C and sent out for analysis.

Statistical Analysis

All statistical tests were performed using Microsoft Excel software on a personal computer. A single tailed Student's t-test or analysis of variance (ANOVA) was used to compare continuous variables. Values of $p < 0.05$ were considered significant.

Results

Procedural Success

Five of seven dogs underwent successful pump implantation, experienced no surgical complications or mechanical (device) failures, and survived to study termination. Two dogs experienced complications and died before study termination: one died of an air embolus in the coronary artery during the second doxorubicin infusion; the other died of ventricular fibrillation intraoperatively during pump implantation.

Heart Failure Induction

Comparison of echocardiographic and hemodynamic data recorded before the first intracoronary doxorubicin injection and immediately before pump implantation confirmed the efficacy of the heart failure induction protocol (**Table 1**). There was a statistically significant increase in LVDs and LVDd (from 21.9 ± 1.4 mm to 31.5 ± 2.6 mm and from 34 ± 2.0 mm to 40.4 ± 3.0 mm, respectively; $p < 0.05$) and a decline in fractional shortening (FS) (from 35.5 ± 1.5% to 22.0 ± 2.3%; $p < 0.05$). Right ventricular dimensions and function were normal and remained close to baseline levels. Heart rate and LVEDP significantly increased (from 99 ± 3 bpm to 115 ± 10 bpm and from 6.4 ± 1.8 mm Hg to 13.6 ± 2.1 mm Hg, respectively; $p < 0.05$).

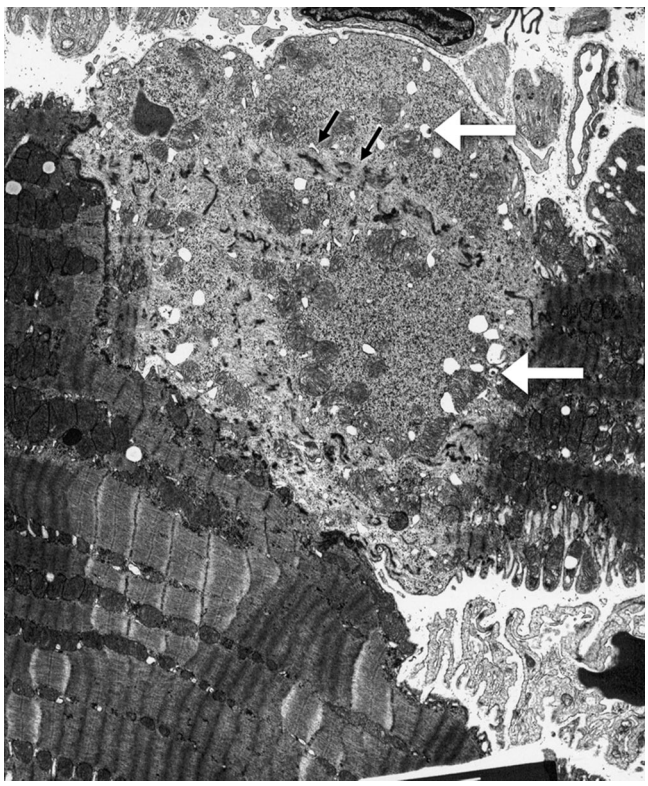

Figure 1. Electron micrograph showing degeneration of isolated cardiac myocytes 4 weeks after fifth and final doxorubicin infusion. Signs of degeneration include myofibril loss, intracytoplasmic vacuoles (some containing membrane whorls) (black arrows), and Z-band widening and splitting (white arrows). Magnification ×2,500.

Table 2. Echocardiographic, Hemodynamic, and Perfusion Data During Pump Support

	Pump Setting (% Support)				
	Pump Off	70NP	100NP	70P	100P
LVDs (mm)	31.5 ± 2.6	22.7 ± 3.6*	20.8 ± 6.5*	23.2 ± 5.1*	20.2 ± 5.3*
LVDd (mm)	40.4 ± 3.0	31.3 ± 2.9*	25.8 ± 6.7*	31.8 ± 4.2*	26.2 ± 4.9*
FS (%)	22.0 ± 2.3	27.8 ± 5.6	20.5 ± 4.9	27.56 ± 8.5	23.4 ± 6.7
HR (bpm)	115 ± 10	108 ± 14	108 ± 13	109 ± 4	109 ± 17
Aortic pressure (mm Hg)					
Systolic	98 ± 11	90 ± 8	75 ± 9*	86 ± 10	78 ± 15*
Diastolic	57 ± 8	64 ± 6	65 ± 8	61 ± 6	55 ± 9
Mean	69 ± 8	73 ± 7	69 ± 9	70 ± 7	64 ± 10
Pulse pressure (mm Hg)	41 ± 16	27 ± 6	10 ± 5*	27 ± 10	21 ± 14
LVP (mm Hg)	94 ± 8	85 ± 10	54 ± 18*	82 ± 11	52 ± 12*
dp/dt_{max} (mm Hg/sec)	2,485 ± 238	2,281 ± 329	1,576 ± 285*	2,293 ± 115	1,531 ± 410*
LVEDP (mm Hg)	13.6 ± 2.1	12 ± 2.7	11.8 ± 2.6	12.2 ± 2.4	11.8 ± 2.2
CO (L/min)	4.17 ± 0.7	3.85 ± 0.7	3.80 ± 0.4	4.10 ± 0.2	3.71 ± 0.4
Pump flow (L/min)	0	2.23 ± 0.36	3.37 ± 0.43**	2.31 ± 0.14	3.47 ± 0.38**
Asc Ao flow (L/min)	3.44 ± 0.3	0.98 ± 0.16*	−0.14 ± 0.3*	0.94 ± 0.11*	−0.24 ± 0.33*
CBF (mL/min)	64 ± 9	51 ± 9	41 ± 12*	56 ± 7.1	44 ± 11*
MVO_2	317 ± 51	221 ± 69*	153 ± 31*	224 ± 25*	137 ± 45*
CBF/MVO_2	0.21 ± 0.04	0.24 ± 0.06	0.27 ± 0.05	0.25 ± 0.03	0.33 ± 0.07*
PAP (mm Hg)	23.2 ± 0.8	23.1 ± 0.6	22.4 ± 0.6	22.9 ± 0.6	22.6 ± 0.5
CVP (mm Hg)	5.2 ± 0.8	5.0 ± 0.6	5.3 ± 0.4	5.1 ± 0.7	5.2 ± 0.7

Values are mean ± SD. Asc Ao, ascending aorta; CBF, coronary blood flow; CO, cardiac output; CVP, central venous pressure; dp/dt, rate of change of left ventricular pressure over time; FS, fractional shortening; HR, heart rate; LVDd indicates left ventricular end-diastolic dimension; LVDs, left ventricular end systolic dimension; LVEDP, left ventricle end diastolic pressure; LVP, left ventricle systolic pressure; MVO_2, myocardial oxygen consumption; NP, nonpulsatile; P, pulsatile; PAP, pulmonary artery pressure.

* $p < 0.05$ *vs.* pump off.

** $p < 0.05$ *vs.* 70 NP or 70 P.

Electron microscopic evaluation of myocardial tissue showed degenerative changes including loss of myofibrils and cytoplasmic vacuolization, as well as atypical myocyte arrangement without signs of disarray (**Figure 1**).

Hemodynamic Assessments

Hemodynamic data are summarized in **Table 2**. The interaction between CO, pump flow, and ascending aortic flow is shown in **Figure 2**. Changes in CBF and MVO_2 are shown in **Figure 3**.

At 70NP, no statistically significant changes were observed in aortic pressures, pulse pressure, LVP, dp/dt_{max}, LVEDP, or CO. The mean pump flow was 2.23 ± 0.36 L/min. The mean contribution of the pump to CO was 54 ± 11%. Compared with baseline (pump off) values, ascending aortic flow and MVO_2 decreased significantly ($p < 0.05$); CBF also decreased but not significantly. The CBF/MVO_2 ratio was not affected. PAP and CVP remained close to baseline levels.

At 100NP, mean AoPs declined progressively from baseline levels (from 98 ± 11 mm Hg to 75 ± 9 mm Hg; $p < 0.05$). Mean AoPd and AoPm also decreased, although the declines were less pronounced and were not statistically significant. Mean aortic pulse pressure decreased significantly from 41 ± 16 mm Hg to 10 ± 5 mm Hg ($p < 0.05$), as did LVP and dp/dt_{max} ($p < 0.05$). Mean LVEDP and CO values slightly decreased but not significantly. Mean pump flow rose gradually from 2.23 ± 0.36 L/min to 3.37 ± 0.43 L/min ($p < 0.05$, *vs.* 70NP). The mean contribution of the pump to CO at 100 NP was 86 ± 6%. The mean blood flow in the ascending aorta dropped significantly from 3.44 ± 0.3 L/min to −0.14 ± 0.3 L/min ($p < 0.05$ *vs.* pump off) and reversed direction toward the aortic valve. Mean CBF decreased from 64 ± 9 ml/min to 41 ± 12 ml/min ($p < 0.05$ *vs.* pump off). The reduction in mean MVO_2 levels (from 317 ± 51 ml/min/kg to 153 ± 31 ml/min/kg) was consistent with the fall in CBF ($p < 0.05$ *vs.* pump off). The ratio of CBF to MVO_2 was well preserved at 100NP. PAP and CVP remained near baseline (pump off) levels.

At 70P, aortic pressures remained close to baseline (pump off) values, and pulse pressure slightly decreased. LVP, dp/dt_{max}, LVEDP, CO, and pump flow measurements did not change significantly. The mean contribution of the pump to

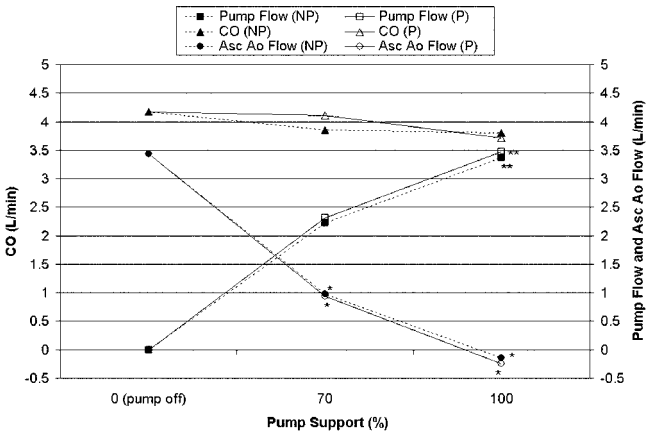

Figure 2. CO, pump flow, and Asc Ao Flow during pump support. CO, cardiac output; Asc Ao Flow, ascending aorta flow; NP, nonpulsatile; P, pulsatile. *$p < 0.05$ *vs*. pump off; **$p < 0.05$ *vs*. 70 NP or 70 P.

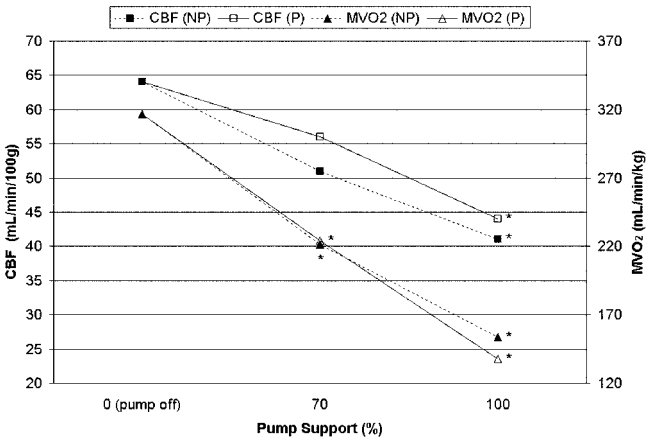

Figure 3. CBF and MVO_2 during pump support. CBF, coronary blood flow; MVO_2, myocardial oxygen consumption; NP, nonpulsatile; P, pulsatile. *$p < 0.05$ *vs*. pump off.

CO was 56 ± 6%. The mean blood flow in the ascending aorta diminished from 3.44 ± 0.3 L/min to 0.94 ± 0.11 L/min ($p < 0.05$ *vs*. pump off). The mean CBF decreased slightly, whereas the mean MVO_2 significantly decreased from 317 ± 51 ml/min/kg to 224 ± 25 ml/min/kg ($p < 0.05$ *vs*. pump off). Nevertheless, the CBF/MVO_2 ratio was not adversely affected. Again, PAP and CVP remained near baseline (pump off) levels.

At 100P, mean AoPs decreased significantly (from 98 ± 11 mm Hg to 78 ± 15 mm Hg; $p < 0.05$ *vs*. pump off). Mean AoPd and AoPm also decreased, but not significantly. Unlike at 100NP, pulse pressure did not significantly decrease at 100P. Mean LVP and dp/dt max both decreased significantly from baseline levels (from 94 ± 8 mm Hg to 52 ± 12 mm Hg and from 2,485 ± 238 mm Hg/sec to 1,531 ± 410 mm Hg/sec, respectively; $p < 0.05$). Mean pump flow increased significantly from 2.31 ± 0.14 L/min to 3.47 ± 0.38 L/min ($p < 0.05$ *vs*. 70P). The mean contribution of the pump to CO was 93 ± 1%. Blood flow in the ascending aorta reversed direction toward the aortic valve at a rate of −0.24 ± 0.33 L/min ($p < 0.05$ *vs*. pump off). CBF and MVO_2 decreased sharply (from 64 ± 9 ml/min to 44 ± 11 ml/min and from 317 ± 51 ml/min/kg to 137 ± 45 ml/min/kg, respectively; $p < 0.05$). Although mean CBF and MVO_2 both decreased gradually, the CBF/MVO_2 ratio significantly increased (from 0.21 ± 0.04 to 0.33 ± 0.07; $p < 0.05$ *vs*. pump off). Again, PAP and CVP remained near baseline (pump off) levels.

Echocardiographic Assessments

At 70NP, LVDs and LVDd were significantly reduced compared with the pump off values (**Table 2**; $p < 0.05$, for both). At 100NP, LVDs and LVDd further decreased (**Table 2**; $p < 0.05$ *vs*. pump off). Similarly, at 70P, LVDs and LVDd significantly decreased (**Table 2**; $p < 0.05$ *vs*. pump off). At 100P, LVDs and LVDd decreased even further ($p < 0.05$ *vs*. pump off). When compared with baseline values, FS, RV dimensions, and wall motion did not change at any experimental setting.

Microsphere Analysis of End Organ Perfusion

The results of microsphere analysis of end organ perfusion are summarized in **Table 3**.

In the left ventricle, blood flow remained near baseline levels at 70NP or 70P. At 100NP, however, blood flow decreased significantly below baseline levels in the posterior and anterolateral epicardial segments, in the anterolateral endocardial segment, and in the subendocardium and subepicardium of the LV free wall, which were calculated as the means of anterolateral and posterior subendocardial and subepicardial blood flow, respectively (**Figure 4**). At 100P, blood flow decreased significantly in the anterolateral epicardium and endocardium and in the subepicardium of the LV free wall (**Figure 4**). In the right ventricle, transmural blood flow decreased gradually, but not significantly, from baseline levels at increasing NP and P settings (**Figure 5**).

Table 3. End Organ Perfusion

	Pump Setting (% Support)				
	Pump Off	70NP	100NP	70P	100P
Left ventricle					
Anterolateral wall					
Epicardium	1.263 ± 0.575	0.952 ± 0.300	0.477 ± 0.199*	0.840 ± 0.18	0.514 ± 0.191*
Endocardium	1.495 ± 0.808	1.096 ± 0.240	0.509 ± 0.271*	0.968 ± 0.21	0.598 ± 0.339*
Posterior wall					
Epicardium	1.302 ± 0.692	1.003 ± 0.329	0.501 ± 0.221*	0.919 ± 0.20	0.590 ± 0.273
Endocardium	1.603 ± 0.981	1.170 ± 0.319	0.573 ± 0.323	1.032 ± 0.26	0.612 ± 0.40
Free wall					
Epicardium	1.282 ± 0.624	0.977 ± 0.624	0.489 ± 0.212*	0.880 ± 0.186	0.552 ± 0.226*
Endocardium	1.549 ± 0.850	1.133 ± 0.269	0.541 ± 0.283*	1.000 ± 0.231	0.605 ± 0.353*
Right ventricle	0.947 ± 0.444	0.831 ± 0.323	0.467 ± 0.200	0.748 ± 0.12	0.539 ± 0.215
Brain					
Cortex	0.493 ± 0.190	0.446 ± 0.182	0.325 ± 0.105*	0.435 ± 0.125	0.352 ± 0.142
Medulla	0.327 ± 0.165	0.348 ± 0.175	0.261 ± 0.177	0.335 ± 0.148	0.265 ± 0.133
Kidney					
Cortex	5.050 ± 1.824	4.819 ± 2.624	2.944 ± 1.372	4.599 ± 2.221	3.409 ± 1.850
Medulla	6.971 ± 3.177	5.778 ± 0.427	3.907 ± 1.973	5.799 ± 1.505	4.291 ± 2.348

Values (mL/min/g) are mean ± SD. NP, nonpulsatile; P, pulsatile.
* $p < 0.05$ *vs.* pump off.

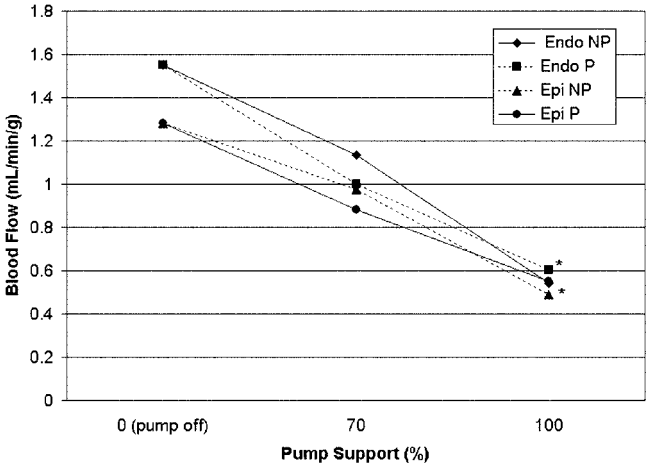

Figure 4. Epi and Endo blood flow in left ventricular free wall. Epi, epicardial; Endo, endocardial; NP, nonpulsatile; P, pulsatile. *$p < 0.05$ *vs*. pump off.

In the brain, cortical blood flow at 70NP decreased, but not significantly, from baseline levels. At 100P, this decrease became statistically significant. At 70P and 100P, the blood flow reduction was less pronounced and not statistically significant. In the corpus medullare, blood flow decreased slightly from baseline levels at increasing NP and P settings.

In the kidneys, blood flow in the renal cortex and medulla gradually decreased, but not significantly, at increasing NP and P settings.

Discussion

Using a prototype LVAD capable of producing both NP and P flow in a canine model of doxorubicin induced heart failure, we showed that flow mode did not significantly affect either hemodynamics or end organ perfusion in the short term.

Our decision to use a model in which dilated cardiomyopathy is induced by intracoronary doxorubicin infusion offered several experimental advantages. First, this model not only mimicked the altered end organ perfusion seen clinically before pump implantation, but it also controlled for the influence of the native healthy heart on pump performance. Thus we were able to assess more precisely the microcirculatory effects of MCS upon poorly perfused end organs (heart, brain, and kidney). Second, intracoronary delivery of doxorubicin allowed us to avoid systemic side effects such as myelosuppression,[12,13] avoid complex surgical interventions including thoracotomy and ligation of coronary arteries,[14–16] and selectively depress LV wall function without severely impairing RV function.[17] Intracoronary delivery also gave us a superior alternative to coronary embolization, which may induce chronic ischemic cardiomyopathy and, consequently, result in higher mortality rates related to myocardial infarction-induced arrhythmias.[18] Third, this model produced hemodynamic and neurohumoral changes that are similar to those seen clinically in patients with heart failure.[19] One disadvantage of the model, however, was its possibility of inducing irreversible myocardial damage, which would have precluded any experimental assessment of myocardial recovery.[20]

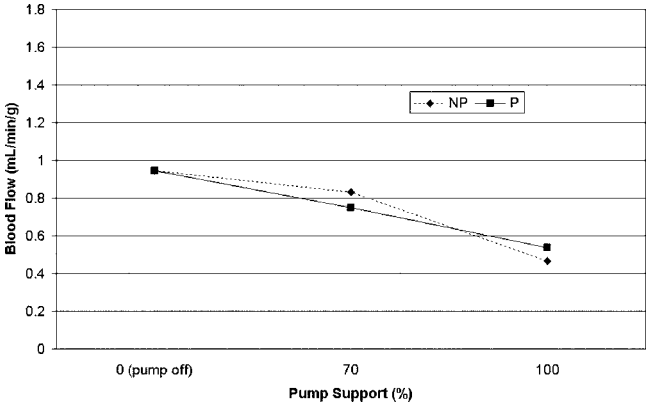

Figure 5. Myocardial (full thickness) blood flow in right ventricle. NP, nonpulsatile; P, pulsatile.

In light of our present results, we believe that our model, and its simple and minimally invasive protocol for inducing heart failure by doxorubicin infusion, can be safely used to evaluate experimentally the short- and long-term end organ effects of LVADs. Indeed, only two dogs died before study termination, one of a coronary air embolism during the doxorubicin induction period and the other of ventricular fibrillation during surgical pump implantation; the five remaining dogs all underwent pump implantation surgery as scheduled. Moreover, as shown by echocardiographic examination of the left ventricle before and after doxorubicin induction, heart failure was successfully induced (**Table 1**).

In contrast with reports of improved FS in normal healthy hearts during long-term LVAD support,[21] our present results suggest that no improvement in FS should be expected immediately after pump implantation in a chronic cardiomyopathy model. In our study, FS remained unchanged even after pump implantation and operation at all experimental settings. However, LVDd and LVDs improved, most likely as a result of effective unloading of the left ventricle.[22–24]

The effect of NP *versus* P flow upon LV function is controversial. Several previous studies suggest that flow with no or reduced pulsatility during acute or chronic NP support does not adversely affect LV function,[3,25,26] whereas other studies with CPB machine or VADs suggest that P support is superior to NP support in preserving major end organ perfusion and metabolism.[27–30] Our present results have shed some light on these two issues. For instance, even though pulse pressure at 70P was 35% lower than at baseline in our study, there was no significant difference between the functional effects of 70P and 70NP flow (**Table 2**). This may have been related to partial unloading of the left ventricle that allowed blood to eject through the aortic valve, thus preserving aortic pulsatility. Nor was there any significant decrease in pulse pressure at 100P. At 100NP, however, the pulse pressure significantly narrowed, presumably as a result of extensive unloading of the left ventricle and impaired aortic valve opening.[23]

Although blood flow through the pump is continuous throughout the cardiac cycle, aortic blood flow remains partially pulsatile. This is because of the contribution of left ventricular contractions, which increases the inlet pressure of the pump during systole (**Figure 6, A and B**). On the other hand, the aortic pressure and pump flow waveforms observed during pulsatile pump support were irregular and different from those

of the natural heart (**Figure 6, C and D**). This phenomenon was probably related to the independent pulse rate of the pump, which was not electrocardiography (ECG) triggered, and one might even speculate that some degree of negative interference may have affected cardiac hemodynamics and end organ microcirculation.

The gradual decrease in dp/dt_{max} that we observed at increasing levels of pump support has been noted before[22,23] and may be attributed to delayed LV relaxation secondary to extensive LV unloading, particularly at 100% of pump support. In fact, the gradual decrease in LVP with increasing pump support, whether NP or P, may lead to a decrease in myocardial work.[31]

Even though the decrease in CBF that we observed was more pronounced in NP mode than in P mode, this did not adversely affect the MVO_2 of the left ventricle (**Figure 3**). In fact, the continuous decrease in CBF (*i.e.*, myocardial perfusion) at increasing levels of pump support (*i.e.*, increasing levels of LV unloading) and in different flow modes paralleled the continuous decrease in the reduced energy demand of the myocardium (MVO_2) secondary to decreased myocardial work and LV wall tension. This was consistent with the findings of previous studies.[6,32,33] Moreover, the increase in CBF/MVO_2 ratio at increasing levels of pump support suggested that the pump did not cause any iatrogenic ischemia of the left ventricle when operating in either NP or P mode.

The gradual decrease in total subendocardial and subepicardial blood flow in the LV free wall that we observed at increasing levels of pump support was consistent with the decrease in CBF and myocardial energy demand. The endocardial/epicardial ratio remained constant as pump support increased, and there was no marked difference in regional perfusion patterns between NP or P flow modes. Yet, even though LV hemodynamics were not altered during our 4 hour study period, longer-term studies are needed to assess the recovery potential of myocytes and the adaptive response of the myocardium to chronically reduced perfusion conditions during prolonged periods of LVAD support.

The effects of P and NP flow upon cerebral perfusion have been studied previously. A number of groups have used hypothermic cardiopulmonary bypass models but produced inconsistent results.[34–37] Others have shown cerebral circulation not to be adversely affected by continuous (*i.e.*, NP) pump flow

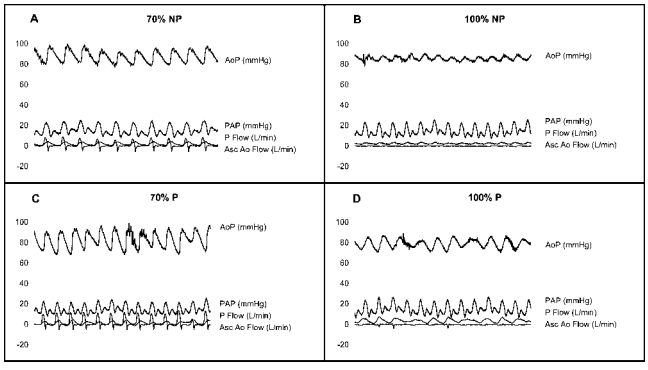

Figure 6. Waveforms of AoP, PAP, P Flow, and Asc Ao Flow during pump support. AoP, aortic pressure; PAP, pulmonary artery pressure; P Flow, pump flow; Asc Ao Flow, ascending aortic flow; NP, nonpulsatile; P, pulsatile.

in either acute[38] or chronic[7] settings and cerebral autoregulation to be well maintained in both. In the present study, however, we found that regional perfusion of the cerebral cortex and medulla gradually decreased with increasing pump support until the decrease finally became significant in the cerebral cortex at 100NP. These findings are inconsistent with several previously published reports.[38–40] This inconsistency may be related to differences in measurement techniques (microsphere analysis[4] *vs.* tissue flow meters[39] or behavioral observation[7]), model (chronic dilated cardiomyopathy[17] *vs.* acute cardiogenic shock[6]), or device (a single bimodal pump implanted in the same animal[41] *vs.* different pumps with different flow modes implanted in different animals[6,7]). It may even be related to anesthesia induced alterations in the cerebral autoregulatory system.

There have been many studies of kidney perfusion during circulatory support. In an ovine model of acute myocardial ischemia, Meyns *et al.*[4] observed an insignificant decrease in cortical and medullar perfusion during both P and NP support. In another experimental study, Saito *et al.*[7] showed that chronic NP circulatory support induced no functional or histologic changes in the kidneys. Many other experimental studies have shown the superiority of P over NP support.[39,42,43] Most of those studies, however, were performed in acute cardiogenic shock models, in which the renal autoregulatory (neurohumoral) mechanisms may have differed from those that would be seen in comparable chronic heart failure models.[44–46] In the present study, both NP and P support in our animal model of chronic heart failure reduced kidney perfusion to similar extents in the short term. It remains to be seen whether the long-term adaptive responses to P and NP circulatory support in these two types of models differ substantially from the short-term responses. Furthermore, it is impossible to extrapolate these animal findings to the human patient with chronic heart failure and its multiple variables. For instance, the chronic pulmonary hypertension that accompanies chronic heart failure in humans is not reproduced in this or any other experimental animal model.

Others have reported that, under NP flow conditions, the velocity of erythrocytes in capillaries and the number of perfused capillaries decrease in direct proportion to the impairment of basal and flow stimulated release of nitric oxide from the microvascular endothelium.[47] In our study, we did not observe any significant difference in end organ regional perfusion between the flow modes; however, we do note here that the NP and P modes at different pump support levels were maintained for only 10 minutes before measurements were taken. Perhaps the 10 minute time period has not been long enough to allow the pump flow mode to affect erythrocyte flow patterns and microsphere distribution in the end organs. Therefore, further studies are needed to clarify the short- and long-term effects of NP and P flow upon cerebral and other end organ microcirculation.

The effects of mechanical LV support upon the unassisted right ventricle have not been fully documented. Several investigators have argued that ventricular septal shifting or increased venous return that reportedly occurs during LVAD support may detrimentally affect RV function.[48–50] Others have suggested that LVAD support may exacerbate a preexisting state of RV ischemia or induce it.[51] In general, experimental studies have not shown any effect of LVAD support upon

the function of a nonischemic right ventricle.[51,52] In an experimental study using healthy pig hearts supported by a pulsatile LVAD operating in synchronous (ECG triggered) and asynchronous (volume triggered) modes, Hendry *et al.*[53]observed a gradient of regional blood flow within the right ventricle along the right coronary artery in both modes. They also observed that this gradient did not cause RV dysfunction and that perfusion throughout the LV septum and free wall remained almost constant. In our present study, we observed that RV myocardial perfusion was adversely affected at increasing levels of pump support, regardless of flow mode, but we could not say whether this was due to the pump's flow properties. Consequently, the potential effects of long-term P and NP pump support upon RV perfusion, with or without increased venous return or septal shift, should be tested in larger numbers of animal subjects in appropriate nonischemic and ischemic models.

Our study did have some limitations. Although performed in a doxorubicin-induced chronic dilated cardiomyopathy model, it did not produce findings upon which we could base any definitive conclusions about the long-term effects of continuous or pulsatile flow upon the end organ (heart, kidney and brain) microcirculation. Instead, our findings reflected the acute setting changes that were made when autoregulatory mechanisms were at work. Moreover, it was not possible to quantify or standardize the effects of the anesthesia performed and surgical trauma incurred during pump implantation, although the baseline hemodynamics immediately after pump implantation were normal. It is also not clear what effect, if any, the choice of graft anastomosis site (*i.e.*, ascending *vs.* descending aorta) had upon aortic and myocardial blood flow properties. Further studies in this regard are warranted.

Conclusion

The present results suggest that hemodynamics and end organ function are not differentially affected by LVAD flow mode in a canine model of doxorubicin-induced congestive heart failure. Larger, longer-term studies are warranted to confirm the validity of these findings in chronic circulatory assist and to establish the usefulness of this animal model.

References

1. Frazier OH, Rose EA, Oz MC, *et al*: Multicenter clinical evaluation of the HeartMate vented electric left ventricular assist system in patients awaiting heart transplantation. *J Thorac Cardiovasc Surg* 122: 1186–1195, 2001.
2. Frazier OH, Myers TJ: Left ventricular assist system as a bridge to myocardial recovery. *Ann Thorac Surg* 68: 734–741, 1999.
3. Frazier OH, Myers TJ, Westaby S, Gregoric ID: Use of the Jarvik 2000 left ventricular assist system as a bridge to heart transplantation or as destination therapy for patients with chronic heart failure. *Ann Surg* 237: 631–636, 2003.
4. Meyns B, Nishimura Y, Racz R, Jashari R, Flameng W: Organ perfusion with Hemopump device assistance with and without intraaortic balloon pumping. *J Thorac Cardiovasc Surg* 114: 243–253, 1997.
5. Baldwin RT, Radovancevic B, Conger JL, *et al*: Peripheral organ perfusion augmentation during left ventricular failure: A controlled bovine comparison between the intraaortic balloon pump and the Hemopump. *Tex Heart Inst J* 20: 275–280, 1993.
6. Merhige ME, Smalling RW, Cassidy D, *et al*: Effect of the hemopump left ventricular assist device on regional myocardial perfusion and function: Reduction of ischemia during coronary occlusion. *Circulation* 80: III158–166, 1989.
7. Saito S, Westaby S, Piggot D, *et al*: End-organ function during chronic nonpulsatile circulation. *Ann Thorac Surg* 74: 1080–1085, 2002.
8. Henry WL, DeMaria A, Gramiak R, *et al*: Report of the American Society of Echocardiography Committee on nomenclature and standards in two-dimensional echocardiography. *Circulation* 62: 212–217, 1980.
9. Sidi A, Rush W: An alternative to radioactive microspheres for measuring regional myocardial blood flow, Part 1: Colored microspheres. *J Cardiothorac Vasc Anesth* 10: 368–373, 1996.
10. Versieck J, Vanballenberghe L: Determination of tin in human blood serum by radiochemical neutron activation analysis. *Anal Chem* 63: 1143–1146, 1991.
11. Reinhardt CP, Dalhberg S, Tries MA, Marcel R, Leppo JA: Stable labeled microspheres to measure perfusion: Validation of a neutron activation assay technique. *Am J Physiol Heart Circ Physiol* 280: H108–116, 2001.
12. Gralla EJ, Fleischman RW, Luthra YK, Stadnicki SW: The dosing schedule dependent toxicities of adriamycin in beagle dogs and rhesus monkeys. *Toxicology* 13: 263–273, 1979.
13. Tomlinson CW, McGrath GM, McNeill JH: Adriamycin cardiomyopathy: Pathological and membrane functional changes in a canine model with mild impairment of left ventricular function. *Can J Cardiol* 2: 368–374, 1986.
14. Armstrong PW, Stopps TP, Ford SE, de Bold AJ: Rapid ventricular pacing in the dog: Pathophysiologic studies of heart failure. *Circulation* 74: 1075–1084, 1986.
15. Millner RW, Mann JM, Pearson I, Pepper JR: Experimental model of left ventricular failure. *Ann Thorac Surg* 52: 78–83, 1991.
16. Magovern JA, Christlieb IY, Badylak SF, Lantz GC, Kao RL: A model of left ventricular dysfunction caused by intracoronary adriamycin. *Ann Thorac Sur* 53: 861–863, 1992.
17. Toyoda Y, Okada M, Kashem MA: A canine model of dilated cardiomyopathy induced by repetitive intracoronary doxorubicin administration. *J Thorac Cardiovasc Surg* 115: 1367–1373, 1998.
18. Sabbah HN, Stein PD, Kono T, *et al*: A canine model of chronic heart failure produced by multiple sequential coronary microembolizations. *Am J Physiol* 260: H1379–1384, 1991.
19. Levine TB, Francis GS, Goldsmith SR, Simon AB, Cohn JN: Activity of the sympathetic nervous system and renin-angiotensin system assessed by plasma hormone levels and their relation to hemodynamic abnormalities in congestive heart failure. *Am J Cardiol* 49: 1659–1666, 1982.
20. Zhou S, Starkov A, Froberg MK, Leino RL, Wallace KB: Cumulative and irreversible cardiac mitochondrial dysfunction induced by doxorubicin. *Cancer Res* 61: 771–777, 2001.
21. Nasu M, Okada Y, Fujiwara H, *et al*: Transesophageal echocardiographic findings of intracardiac events during cardiac assist. *Artif Organs* 14: 377–381, 1990.
22. Saito A, Shiono M, Orime Y, *et al*: Effects of left ventricular assist device on cardiac function: Experimental study of relationship between pump flow and left ventricular diastolic function. *Artif Organs* 25: 728–732, 2001.
23. Tuzun E, Eya K, Chee HK, *et al*: Myocardial hemodynamics, physiology, and perfusion with an axial flow left ventricular assist device in the calf. *ASAIO J* 50: 47–53, 2004.
24. Westaby S, Jin XY, Katsumata T, Taggart DP, Coats AJ, Frazier OH: Mechanical support in dilated cardiomyopathy: Signs of early left ventricular recovery. *Ann Thorac Surg* 64: 1303–1308, 1997.
25. Finlayson DC: Con: Nonpulsatile flow is preferable to pulsatile flow during cardiopulmonary bypass. *J Cardiothorac Anesth* 1: 169–170, 1987.
26. Potapov EV, Loebe M, Nasseri BA, *et al*: Pulsatile flow in patients with a novel nonpulsatile implantable ventricular assist device. *Circulation* 102 (Suppl. 3): III183–187, 2000.
27. Shevde K, DeBois W: Pro: Pulsatile flow is preferable to nonpulsatile flow during cardiopulmonary bypass. *J Cardiothorac Anesth* 1: 165–168, 1987.
28. Taylor KM, Bain WH, Davidson KG, Turner MA: Comparative

clinical study of pulsatile and non-pulsatile perfusion in 350 consecutive patients. *Thorax* 37: 324–330, 1982.
29. Fukae K, Tominaga R, Tokunaga S, Kawachi Y, Imaizumi T, Yasui H: The effects of pulsatile and nonpulsatile systemic perfusion on renal sympathetic nerve activity in anesthetized dogs. *J Thorac Cardiovasc Surg* 111: 478–484, 1996.
30. Toda K, Tatsumi E, Taenaka Y, Masuzawa T, Takano H: Impact of systemic depulsation on tissue perfusion and sympathetic nerve activity. *Ann Thorac Surg* 62: 1737–1742, 1996.
31. Shiiya N, Zelinsky R, Deleuze PH, Loisance DY: Effects of Hemopump support on left ventricular unloading and coronary blood flow. *ASAIO Tran* 37: M361–M362, 1991.
32. Kono S, Nishimura K, Nishina T, *et al*: Autosynchronized systolic unloading during left ventricular assist with a centrifugal pump. *J Thorac Cardiovasc Surg* 125: 353–360, 2003.
33. Goldstein AH, Pacella JJ, Clark RE: Predictable reduction in left ventricular stroke work and oxygen utilization with an implantable centrifugal pump. *Ann Thorac Surg* 58: 1018–1024, 1994.
34. Henze T, Stephan H, Sonntag H: Cerebral dysfunction following extracorporeal circulation for aortocoronary bypass surgery: No differences in neuropsychological outcome after pulsatile versus nonpulsatile flow. *Thorac Cardiovasc Surg* 38: 65–68, 1990.
35. Lodge AJ, Undar A, Daggett CW, Runge TM, Calhoon JH, Ungerleider RM: Regional blood flow during pulsatile cardiopulmonary bypass and after circulatory arrest in an infant model. *Ann Thorac Surg* 63: 1243–1250, 1997.
36. Sapire KJ, Gopinath SP, Farhat G, *et al*: Cerebral oxygenation during warming after cardiopulmonary bypass. *Crit Care Med* 25: 1655–1662, 1997.
37. Sanderson JM, Wright G, Sims FW: Brain damage in dogs immediately following pulsatile and non-pulsatile blood flow in extracorporeal circulation. *Thorax* 27: 275–286, 1972.
38. Kashiwazaki S: Effects of artificial circulation by pulsatile and non-pulsatile flow on brain tissues. *Ann Thorac Cardiovasc Surg* 6: 389–396, 2000.
39. Sezai A, Shiono M, Orime Y, *et al*: Major organ function under mechanical support: Comparative studies of pulsatile and nonpulsatile circulation. *Artif Organs* 23: 280–285, 1999.
40. Tsutsui T, Sutton C, Harasaki H, Jacobs G, Golding L, Nose Y: Idioperipheral pulsation during nonpulsatile biventricular bypass experiments. *ASAIO Trans* 32: 263–268, 1986.
41. Nishinaka T, Tatsumi E, Nishimura T, *et al*: Effects of reduced pulse pressure to the cerebral metabolism during prolonged nonpulsatile left heart bypass. *Artif Organs* 24: 676–679, 2000.
42. Nakata K, Shiono M, Orime Y, *et al*: Effect of pulsatile and nonpulsatile assist on heart and kidney microcirculation with cardiogenic shock. *Artif Organs* 20: 681–684, 1996.
43. Sezai A, Shiono M, Orime Y, *et al*: Microcirculation of kidney and skin during left ventricular assisted circulation: Comparative studies of pulsatile and nonpulsatile assists. *Jpn J Thorac Cardiovasc Surg* 46: 1239–1246, 1998.
44. Pinto YM, de Smet BG, van Gilst WH, *et al*: Selective and time related activation of the cardiac renin-angiotensin system after experimental heart failure: relation to ventricular function and morphology. *Cardiovasc Res* 27: 1933–1938, 1993.
45. Redfield MM, Edwards BS, Heublein DM, Burnett JC Jr: Restoration of renal response to atrial natriuretic factor in experimental low-output heart failure. *Am J Physiol* 257: R917–923, 1989.
46. Charloux A, Piquard F, Doutreleau S, Brandenberger G, Geny B: Mechanisms of renal hyporesponsiveness to ANP in heart failure. *Eur J Clin Invest* 33: 769–778, 2003.
47. Baba A, Dobsak P, Saito I, *et al*: Microcirculation of the bulbar conjunctiva in the goat implanted with a total artificial heart: effects of pulsatile and nonpulsatile flow. *ASAIO J* 50: 321–327, 2004.
48. Holman WL, Bourge RC, Fan P, Kirklin JK, Pacifico AD, Nanda NC: Influence of left ventricular assist on valvular regurgitation. *Circulation* 88: II309–I318, 1993.
49. Moon MR, Castro LJ, DeAnda A, *et al*: Right ventricular dynamics during left ventricular assistance in closed-chest dogs. *Ann Thorac Surg* 56: 54–66, 1993.
50. Farrar DJ, Compton PG, Hershon JJ, Fonger JD, Hill JD: Right heart interaction with the mechanically assisted left heart. *World J Surg* 9: 89–102, 1985.
51. Shuman TA, Palazzo RS, Jaquiss RB, *et al*: A model of right ventricular failure after global myocardial ischemia and mechanical left ventricular support. *ASAIO Trans* 37: M212–213, 1991.
52. Chow E, Brown CD, Farrar DJ: Effects of left ventricular pressure unloading during LVAD support on right ventricular contractility. *ASAIO J* 38: M473–476, 1992.
53. Hendry PJ, Nathan H, Rajagopalan K: Right ventricular blood flow during left ventricular support in an experimental porcine model. *Ann Thorac Surg* 61: 1199–1204, 1996.